Agronomy Research **17**(X), xxx–ccc, 2019
https://doi.org/10.15159/AR.19.041

The influence of changing hydropower potential on performance parameters of pump in turbine mode

M. Polák

Czech University of Life Sciences in Prague, Faculty of Engineering, Kamýcká 129, CZ16521 Praha 6, Czech Republic
Correspondence: karel@tf.czu.cz

Abstract. Various types of hydromotors that enable energy recovery simultaneously with the required pressure reduction can be used in the field of fluid pumping systems. Similar principle is applied, for example, in the case of use of hydrodynamic pumps in turbine mode (PAT), which are also used as an alternative to conventional turbines in small hydropower plants. However, these pumps do not usually have the possibility of regulating hydraulic parameters, as it is common with conventional turbines. This specific feature needs to be taken into account, when designing such system. Article analyses computational methods for the conversion of the performance characteristics and compares these results with experimentally measured data on a particular pump in turbine mode. The results indicated that conversion can be well used in practice to predict outputs as well as to determine the optimum total head and flowrate to ensure maximum efficiency of PAT operation. Further computations were influenced by deviations resulting from the change in efficiency during PAT operation.

Key words: pump as turbine (PAT), total head, flowrate, power output, efficiency.

INTRODUCTION

In recent decades, interest in pump as turbine (PAT) technology has been renewed and it has been significantly used in remote area power supply installations, both on- and off-grid (Giosio et al., 2015). The use of hydraulic pumps operating as turbines offers several advantages with respect to conventional turbines. The major advantages are its low investment costs and market accessibility. Small centrifugal pumps operating as turbines with an output of 5 kW or less are also a low-cost alternative to crossflow turbines even in small hydropower plants. Another application for pumps as turbines is in fluid supply lines, where pressure reducing valves are often used to control supply pressure (Williams, 1996). The excess head can be exploited for hydropower generation (Pugliese et al., 2016). Control valves are placed within the water distribution network in order to face large variations in altitudes or to dissipate any residual head at the end of the pipeline (Liberatore & Sechi, 2009). In all these cases, a limited variability of flowrates and available head drop is observed and traditional hydropower plants and design criteria can be conveniently used (Afshar et al., 1990). On the contrary, the water regime presents a large variability in water distribution network, because flowrate and pressure head depends on user's demand (Fontana et al., 2012; Carravetta et al., 2013).

However, the possibility of predicting the performance parameters of a pump as a turbine and of selecting the suitable machine for a given hydropower site is still an open issue (Barbarelli et al., 2017; Polák, 2017). A major disadvantage of PAT is its extremely poor performance apart from the best efficiency point (BEP) due to the fixed internal geometry and absence of flow regulation. Various authors have provided, with positive results, a number of relatively simple modifications such as impeller tip and hub/shroud rounding in order to increase overall PAT performance (Singh, 2005; Singh & Nestmann, 2011; Derakhshan et al., 2009; Jain et al., 2015). However, the rapid efficiency drop-off at off-design conditions remains an inherent and major limitation of PAT (Giosio et al., 2015).

The average conversion efficiency was also estimated, both for the overall system and for PAT. It was found that, from an overall perspective, the water distribution network potential is usually rather unexploited, with the exception of one case that had a conversion efficiency of 39%. In fact, the PAT itself usually runs at "acceptable" efficiency values (up to 59%) (Venturini et al., 2017).

MATERIALS AND METHODS

Parameters of hydrodynamic pumps in turbine operation

When comparing the pump and turbine operation, the optimal parameters differ. For turbine pump operation, the same circumferential velocity $|u_P| = |u_T|$, or the same shaft speed $|n_P| = |n_T|$ as for pump operation is usually required. It is because of the use of synchronous motors, which can be operated in a generator mode, and also because the production of electric power must respect the frequency of the grid. The kinematic conditions in the impeller during pump and turbine operation is shown by the velocity triangles in Fig. 1. The dashed lines represent velocity triangle for pump mode, the grey lines show velocity triangle for reversed turbine mode. Vectors u_P, u_T represent circumferential blade velocity at pump and turbine mode, respectively. Vectors c_P, c_T are absolute velocities of fluid and finally vectors w_P, w_T are relative velocities of fluid (relating blade rotation) at pump and/or turbine mode.

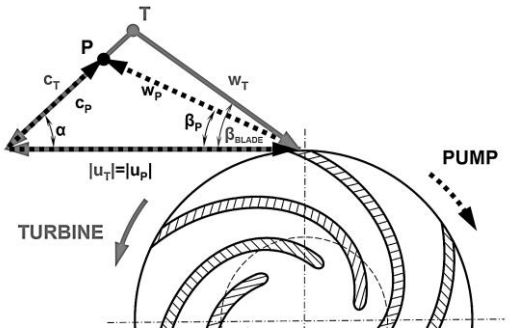

Figure 1. Kinematic conditions during pump and turbine operation.

Due to the diffuser flow of fluid through the impeller during pump operation, the fluid flow is less curved than the angle of the impeller blades at the outside diameter of the impeller ($\beta_P < \beta_{BLADE}$) so that during the shock-free flow, the velocity triangle at the outer diameter of the impeller meets at point P (Capurso et al., 2018). In the case of turbine operation, the flow of the fluid inlet into the impeller is identical to the angle of the impeller blade β_{BLADE}. To avoid the shock of the fluid entering the impeller, the vectors of the velocity triangle of the turbine operation must be joined at point T. Since the height of the velocity triangles is proportional to the flow Q and the absolute velocity

of the fluid c is the total head H_T, the main parameters of the optimum pump turbine operation are the following: $Q_T > Q_P$, $H_T > H_P$ (Bláha et al., 2012).

The conversion relations between pump and turbine mode, i.e. between Q_P and Q_T, or between H_P and H_T vary (Polák, 2018). Their overview is presented in Table 1.

Table 1. Conversion relations according to various authors

Author	Source, Year	Head ratio H_T/H_P	Flowrate ratio Q_T/Q_P	Remarks
Stepanoff	(Stepanoff, 1957)	$\frac{1}{\eta_P}$	$\frac{1}{\sqrt{\eta_P}}$	Accurate for Ns = 40÷60
Childs	(Childs, 1962)	$\frac{1}{\eta_P}$	$\frac{1}{\eta_P}$	-
Hancock	(Hancock, 1963)	$\frac{1}{\eta_T}$	$\frac{1}{\eta_T}$	-
Grover	(Grover, 1980)	$2.693 - 0.0229N_{sT}$	$2.379 - 0.0264N_{sT}$	Applied for Ns = 10÷50
Hergt	(Lewinsky-Keslitz, 1987)	$1.3 - \frac{6}{N_{qT} - 3}$	$1.3 - \frac{1.6}{N_{qT} - 5}$	-
Sharma	(Sharma, 1985)	$\frac{1}{{\eta_P}^{1.2}}$	$\frac{1}{{\eta_P}^{0.8}}$	Accurate for Ns = 40÷60
Schmiedl	(Schmiedl, 1988)	$-1.4 + \frac{2.5}{\eta_P}$	$-1.5 + \frac{2.4}{{\eta_P}^2}$	-
Alatorre-Frenk	(Alatorre-Frenk, 1994)	$\frac{1}{0.85{\eta_P}^5 + 0.385}$	$\frac{0.85{\eta_P}^5 + 0.385}{2{\eta_P}^{9.5} + 0.205}$	-
Güllich-volute	(Güllich, 2008)	$\frac{2.4}{{\eta_P}^2} - 1.5$	$\frac{2.5}{\eta_P} - 1.4$	-

Theoretical methods are quite comprehensive but they are difficult to be applied in practice because they need very detailed geometric information, which are available only to manufacturers (Stefanizzi et al., 2017). It is concluded, that experimental investigations are still indispensable when an exact knowledge of turbine characteristics is required (Kramer et al., 2018). Experimental verification has shown that some methods (e.g. Childs' method) differ significantly from reality, while others (e.g. Stepanoff's method) show small relative differences (Frosima et al., 2017).

Correctly designed conversion ensures maximum machine operation efficiency but only with nominal (design) parameters. However, in actual operation the Q_T flowrate and the H_T gradient changes and so does the shape of the velocity triangles. Thus the vectors of individual velocities do not form a closed triangle. This indicates a speed shock, resulting in a reduction in efficiency. For conventional turbines, this can be avoided by changing the geometry of the flow parts - by turning the guide blades or impeller blades. However, pumps in turbine mode do not have blade control in the vast majority of cases. The solution can only be sought in the change of the circumferential velocity, i.e. the shaft speed. This can be done for example by implementing gears or frequency inverters. In this way, the magnitude of the vectors changes, but the geometric similarity of the velocity triangles remains maintained (α = const., β_{BLADE} = const.). The explanation is presented in Fig. 2. The vectors c_{Tm} and c_{Tu} are projections of absolute velocity to meridional and tangential direction, respectively, corresponding to design (nominal) parameters. After changing the parameters (in this case increasing flowrate

and total head), the corresponding vectors are marked c_{Tm*} and c_{Tu*}. If the geometrical similarity of the triangles is maintained, the speed shock does not occur and the efficiency of the machine is not reduced.

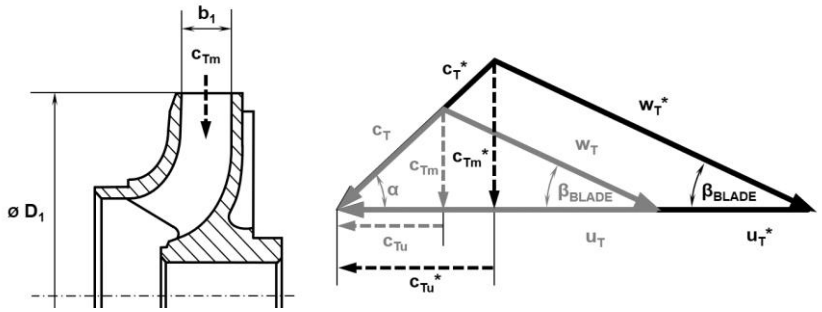

Figure 2. The change of kinematic conditions during turbine operation.

Conversion relations of hydraulic machine parameters

Based on the above assumption of the geometric similarity of the velocity triangles, a change of the operating parameters of PAT can be calculated (Melichar, 2007). The flow of the fluid through the inlet of the impeller at the nominal parameters Q_T (see Fig. 2, the grey triangle) and at the changed parameters Q_T* (see Fig. 2, the black triangle) comes from the continuity equations

$$Q_T = c_{Tm} \cdot S_1 = c_{Tm} \cdot \pi \cdot D_1 \cdot b_1 \text{ and } Q_T^* = c_{Tm}^* \cdot S_1 = c_{Tm}^* \cdot \pi \cdot D_1 \cdot b_1 \qquad (1)$$

By dividing equations (1) Q_T*/ Q_T, provided: π, D_1, b_1 = const., we get

$$Q_T^* = Q_T \cdot \frac{c_{Tm}^*}{c_{Tm}} \qquad (2)$$

The meridional component of the absolute velocity c_{Tm} is the rate of absolute velocity c, which is given by the total head of the turbine. The same applies for c_{Tm}^* at changed parameters. The absolute speed also determines the turbine impeller speed or shaft speed N_T:

$$c_{Tm} \approx c_T \approx N_T \text{ and } c_{Tm}^* \approx c_T^* \approx N_T^* \qquad (3)$$

From using the relation (3) in Eq. (2), we get:

$$Q_T^* = Q_T \cdot \frac{N_T^*}{N_T} \qquad (4)$$

It follows from equation (4) that if the flowrate changes from nominal value Q_T to value Q_T*, it is necessary to change the shaft speed, in order to maintain the geometric similarity of the velocity triangle, to:

$$N_T^* = N_T \cdot \frac{Q_T^*}{Q_T} \qquad (5)$$

The total head or the specific energy at the turbine nominal parameters Y_T and the changed parameters Y_T* is expressed by the Euler equation, assuming the vortex-free fluid output from the impeller.

$$Y_T = u_T \cdot c_{Tu} \text{ and } Y_T^* = u_T^* \cdot c_{Tu}^* \quad (6)$$

The circumferential velocity of the impeller at the inlet u_T, at a constant diameter D_1, is given only by the shaft speed N_T.

$$u_T = \pi \cdot D_1 \cdot N_T \text{ and } u_T^* = \pi \cdot D_1 \cdot N_T^* \quad (7)$$

Analogously to Eq. (3), the magnitude of the projection of the absolute velocity c_{Tu} is given by the magnitude of the absolute velocity, or the shaft speed.

$$c_{Tu} \approx c_T \approx N_T \text{ and } c_{Tu}^* \approx c_T^* \approx N_T^* \quad (9)$$

By substituting the relations (7) and (8) into equations (6), presuming D_1 = const., we come to:

$$Y_T^* = Y_T \cdot \left(\frac{N_T^*}{N_T}\right)^2 \quad (9)$$

When changing the specific energy, or the total head, it is necessary to change the shaft speed to maintain the optimum efficiency, to:

$$N_T^* = N_T \cdot \sqrt{\frac{Y_T^*}{Y_T}} = N_T \cdot \sqrt{\frac{H_T^*}{H_T}} \quad (10)$$

The power output of the turbine operating with a fluid of density ρ at nominal parameters P_T and changed parameters P_T* is given by equations

$$P_T = Q_T \cdot \rho \cdot Y_T \text{ and } P_T^* = Q_T^* \cdot \rho \cdot Y_T^* \quad (11)$$

By dividing equations (11) P_T^*/P_T and by subsequent modification, we get a relation for power output at changed total head, flowrate and shaft speed

$$P_T^* = P_T \cdot \left(\frac{N_T^*}{N_T}\right)^3 \quad (12)$$

The above procedures can also be used to determine the torque:

$$M_T^* = M_T \cdot \left(\frac{N_T^*}{N_T}\right)^2 \quad (13)$$

The characteristics of the turbine at the changing parameters are given by merging the affine relations (4) and (9) that results in:

$$\frac{Y_T^*}{Y_T} = \left(\frac{Q_T^*}{Q_T}\right)^2 \quad (14)$$

By separating Y*, we get an equation of so-called affine parabola with the vertex at the beginning of the coordinates Y_T*-Q_T*.

$$Y_T^* = \frac{Y_T}{Q_T^*} \cdot (Q_T^*)^2 = k \cdot (Q_T^*)^2 \quad (15)$$

The affine parabola links together points corresponding to maximum efficiency. The optimum operating point of the pump in turbine mode must lie on or very near the affine parabola. The position of the working point is controlled either by throttling at the end of the pressure line or in the bypass of the pump, or by changing the shaft speed by means of a gear or frequency inverter. The speed change follows the maximum efficiency curve or the constant flow requirement – for example to maintain sanitary

flow in the riverbed if the pump is placed at the base outflow of a water reservoir (Melichar et al., 1998).

Experimental verification of model calculations of turbine operation

The above mentioned methodology was verified at the author's workplace on a radial single stage centrifugal META series pump, manufactured in the Czech Republic by company ISH PUMPS Olomouc. The pump's parameters in pump mode, as provided by the manufacturer, are in Table 2.

Table 2. Performance parameters of tested PAT in pump mode

Parameter	Value
Impeller diameter: D_1 [mm]	132
Total head: H_P [m]	5.7
Flowrate: Q_P [l.s^{-1}]	3.8
Shaft speed: N_P [rpm]	1,450
Efficiency: η_P [-]	0.63
Specific speed: N_{qP} [rpm]	24

Verification tests were conducted on a hydraulic circuit in the Fluid Mechanics Laboratory at the Faculty of Engineering, Czech University of Life Sciences Prague. The circuit diagram is shown in Fig. 3.

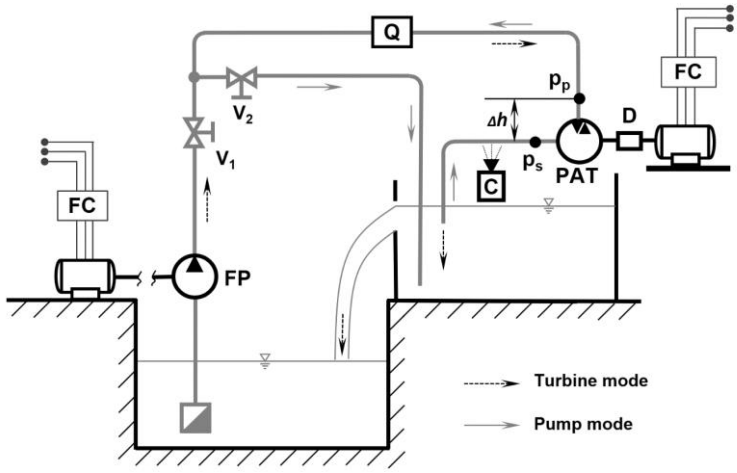

Figure 3. Hydraulic circuit scheme for testing turbines/pumps. Q – flowmeter, FP – feed pump; PAT – tested pump as turbine; V_1, V_2 – control valves; D – dynamometer; FC – frequency inverter; C – camcoder.

The testing circuit consisted of a set of two reservoirs with pipes and control and measuring elements. With this setting, the tested PAT was measured in turbine mode – by closing valve V_2 while regulating valve V_1, the water flowed in the direction of dashed arrows, while the feeding pump (FP) created the hydropower potential for the turbine. The dynamometer (D) with momentum sensor Magtrol TMB 307/41 (accuracy 0.1%) allowed continuous regulation of shaft speed by frequency inverter LSLV0055s100-4EOFNS. This device enabled operation in motor and braking mode. The water flow was measured using an electromagnetic flowmeter (Q) SITRANS F M MAG 5100 W (accuracy 0.5%). Pressures at (p_p) and (p_s) were measured by pressure sensor HEIM 3340 (accuracy 0.5%) installed according to 1st class accuracy requirement (ČSN EN ISO 9906).

RESULTS AND DISCUSSION

The aim of the experimental part of this study was to verify the behaviour of PAT in general piping system, which allows recuperation of energy of a flowing liquid. The main experiment consisted of measuring performance parameters of PAT at six basic hydropower potentials (modes) that simulated changing pipeline system parameters. During the measurement, PAT was gradually loaded from idle speed up to $N_T \approx 500$ min^{-1} in each mode. From the measured values, the performance characteristics were subsequently indicated. Fig. 4 presents the dependence of efficiency on shaft speed. Based on this dependence, BEP, corresponding shaft speed and efficiency was determined for each mode.

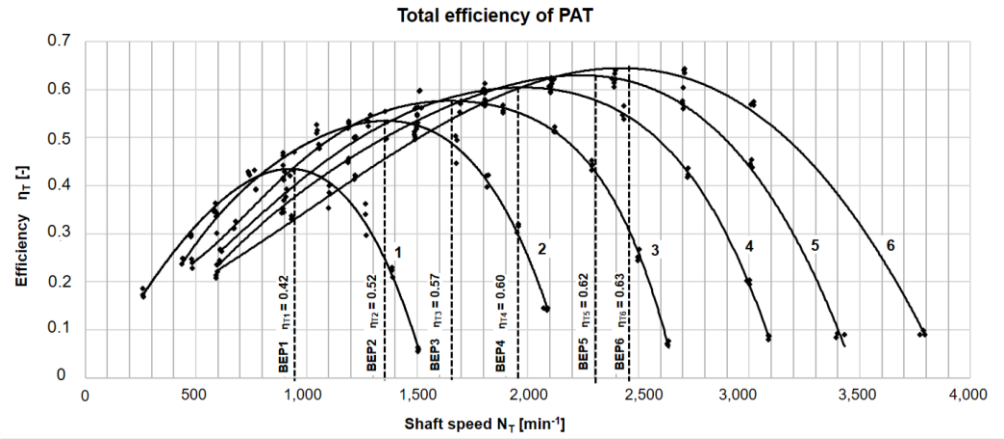

Figure 4. Courses of efficiency in modes 1 to 6 highlighting the optimum (BEP).

The following parameters corresponding to optimum operation at BEP were determined from other characteristics, i.e. flowrate, total head and power output. An overview of all monitored parameters is presented in Table 3.

Table 3. BEP performance parameters of tested PAT

Hydropower potential (mode)	1	2	3	4	5	6
Total efficiency: η_T [-]	0.42	0.52	0.57	0.60	0.62	0.63
Shaft speed: N_T [min^{-1}]	950	1,350	1,650	1,950	2,200	2,450
Flowrate: Q_P [l.s^{-1}]	4.2	5.5	6.5	7.5	8.3	9.1
Total head: H_T [m]	6.1	10.5	15.6	20.6	24.9	30.6
Power output: P_T [kW]	0.11	0.31	0.59	0.96	1.30	1.77

In order to verify the applicability of the predictive relationships (4), (9), (10), (12) and the affine parabola equation (15), other necessary characteristics were determined from the measured values. Fig. 5 presents flowrate (left), or total head (right) dependence on shaft speed. In addition, values for BEP (grey curves) from Table 3 are marked here as well as curves from the predictive calculations (dashed lines) according to equations (4) and (10). The parameters measured in mode 3 were used as input values for the predictive calculations.

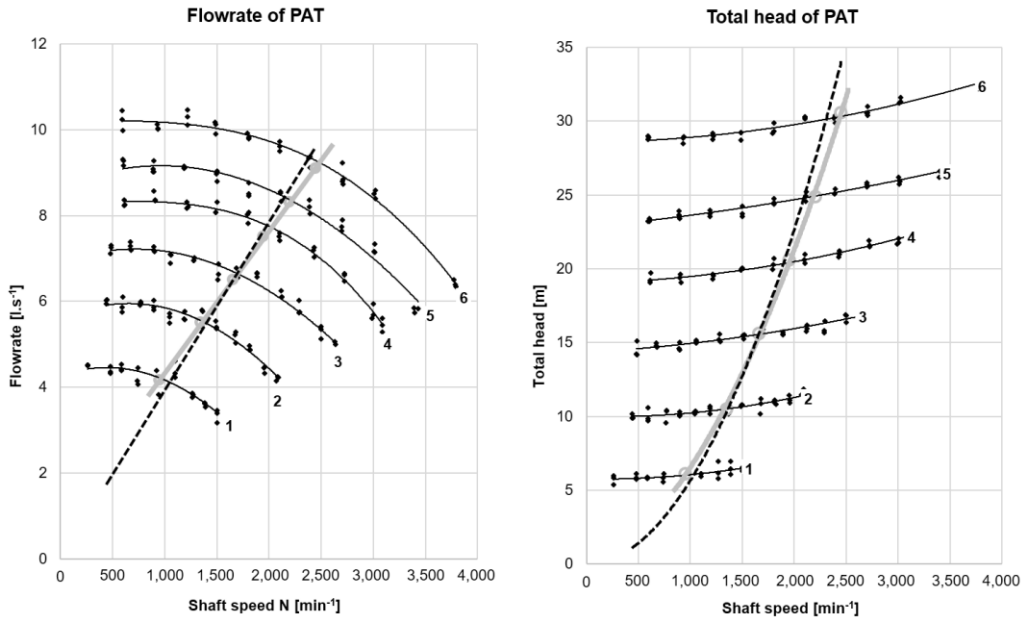

Figure 5. Predictive calculations of flowrate and total head versus reality.

The characteristics presented in Fig. 6 were generated in a similar way. These are dependences of power output on speed (left) and the affine parabola (right), including the measured values (grey curve) and the calculated values (dashed line) for BEP.

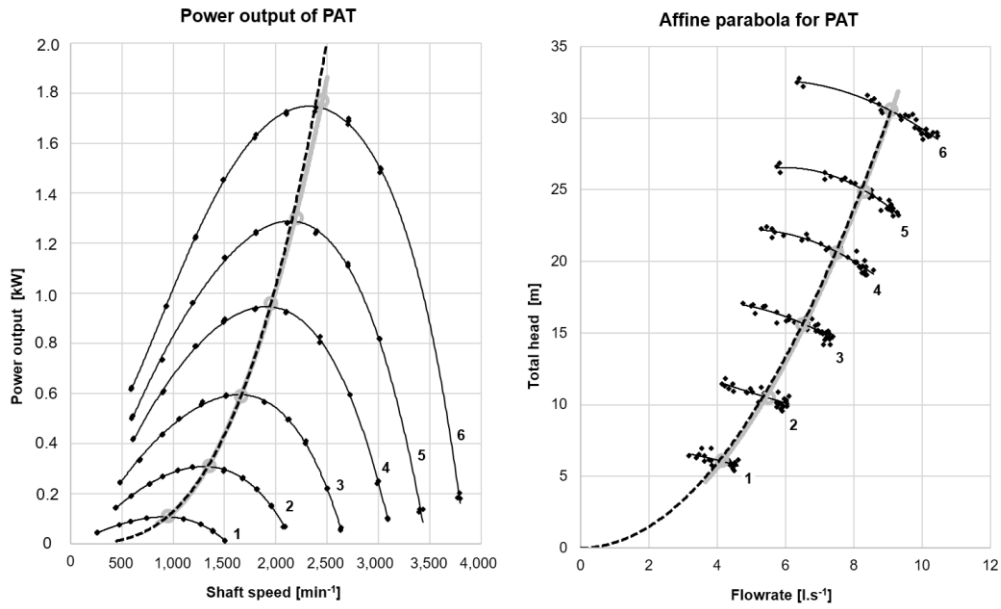

Figure 6. Predictive calculations of power output and affine parabola versus reality.

From the achieved results, the relative deviations of the monitored output parameters were subsequently determined

$$\Delta A = 100 \cdot \frac{A_C - A_R}{A_R} \tag{16}$$

where A_C is calculated value, A_R is measured value. To make the overview of deviations'size and trend clearer, the individual parameters were related to speed and presented in Fig. 7.

The graph in Fig. 7 summarizes the final results of the study and serves to compare the experimentally measured values with the results of the calculation relations for the prediction of flowrate (4), total head (10) and output (12) in relation to shaft speed.

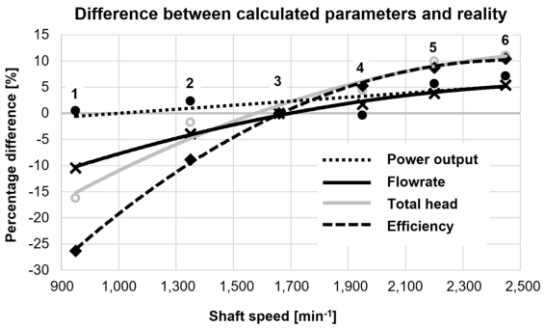

Figure 7. Comparison of predictive calculations with reality.

CONCLUSIONS

Based on the comparison of the results from Fig. 7, the following can be stated: the deviation of the values in mode 3 was zero, since this mode was defined as the base, reference mode.

The deviation of the power output calculation at varying potential was minimal (6% the most), so the conversion ratio (12) can be well used in practice; similarly, the relation for the affine parabola (15) can be used to determine the optimum total head and flowrate to ensure maximum PAT operation efficiency.

The deviations of other variables (flowrate and total head in dependence on speed) gradually increased with increasing distance from reference mode 3; the more so as the difference between the reference and actual value of efficiency increased – from point 3 to the left. On the contrary, where efficiency changed only a little, the other parameters changed in a similar way – from point 3 to the right. To put it simply – the deviation from the predicted efficiency was the cause of the deviation of other parameters. The used model of physical similarity did not include a change in efficiency. But efficiency, especially of small PAT, can be difficult to determine beforehand, the more so if the hydropower potential changes during operation. In order to use PAT efficiently under the conditions of variable potential, it is therefore necessary to focus on this issue more deeply. However, if there is a stable potential provided during PAT operation, all the above calculation methods are reliably applicable.

ACKNOWLEDGEMENTS. This research was supported by project: Activity Proof-of-Concept (No. 99130/1415/4101), Technology Agency of Czech Republic.

REFERENCES

Afshar, A., Jemaa, F. & Marino, M. 1990. Optimization of hydropower plant integration in water supply system. In: *J. Water Res. Plan*. **116**(5), 665–675.

Alatorre-Frenk, C. 1994. Cost minimization in micro hydro systems using pumps-as-turbines, *Ph.D. Thesis*. University of Warwick, 1994.

Barbarelli, S., Amelio, M. & Florio, G. 2017. Experimental activity at test rig validating correlations to select pumps running as turbines in microhydro plants. In: *Energy conversion and Management* **149**, 781–797.

Bláha, J., Melichar, J. & Mosler, P. 2012. Contribution to the use of hydrodynamic pumps as turbines. In: *Energetika* **5***/2012*. ISSN 0375-8842 (in Czech).

Capurso, T., Stefanizzi, M., Torresi, M., Pascazio, G., Caramia, G., Camporeale, S., Fortunato, B., Bergamini, L. 2018. How to Improve the Performance Prediction of a Pump as Turbine by Considering the Slip Phenomenon. In: *Proceedings.* **2**. 683. 10.3390/proceedings2110683.

Carravetta, A., del Giudice, G., Fecarotta, O. & Ramos, H.M. 2013. PAT design strategy for energy recovery in water distribution networks by electrical regulation. In: *Energies* **6**(1), 411–424.

Childs, S.M. 1962. Convert pumps to turbines and recover HP. *Hydro Carbon Processing and Petroleum Refiner* **41**(10), 173–4.

Derakhshan, S, Mohmmadi, B. & Nourbakhsh, A. 2009. Efficiency improvement of centrifugal reverse pumps. In: *J Fluids Eng* **131**(No. 2). Article ID 021103.

Fontana, N., Giugni, M. & Portolano, D. 2012. Losses reduction and energy production in water-distribution networks. In*: J. Water Res. Plan.* **138**(3), 237–244.

Frosina, E., Buono, D. & Senatore, A. 2017. A performance prediction method for pumps as turbines (PAT) using a computational fluid dynamics (CFD) modeling approach. In: *Energies* **10**(1), 103.

Giosio, D.R., Henderson, A.D., Walker, J.M., Brandner, P.A., Sargison, J.E. & Gautam, P. 2015. Design and performance evaluation of a pump-as-turbine micro-hydro test facility with incorporated inlet flow control. In: *Renewable Energy* **78**, 1–6.

Grover K., M. 1980. *Conversion of pumps to turbines*. Katonah, New York: GSA Inter Corp. pp. 125–138.

Gülich, J.F. 2008. *Centrifugal pumps*. 3rd Edition. Berlin: Springer, 1116 pp., ISBN 978-3-642-40113-8.

Hancock, J.W. 1663. Centrifugal pump or water turbine. *Pipe Line News*, pp. 25–7.

Jain Sanjay, V, Swarnkar Abhishek, Motwani Karan, H & Patel Rajesh, N. 2015. Effects of impeller diameter and rotational speed on performance of pump running in turbine mode. In: *Energy Convers Manage* **89**, 808–24.

Kramer, M., Terheiden, K. & Wieprecht, S. 2018. Pumps as turbines for efficient energy recovery in water supply networks. In: *Renewable Energy* **122**, 17–25.

Liberatore, S. & Sechi, G. 2009. Location and calibration of valves in water distribution networks using a scatter-search meta-heuristic approach. In: *Water Res. Manag.* **23**, 1479–1495.

Lewinsky-Keslitz, H.P. 1987. Pumpen als Turbinen fur Kleinkraftwerke. *Wasserwirtschaft* **77**(10):531–7.

Melichar, J., Vojtek, J. & Bláha, J. 1998. *Small hydro turbines, construction and operation*. ČVUT, Praha, 296 pp. (in Czech).

Melichar, J. & Bláha, J. 2007. Problems of contemporary pumping technology, selected parts. ČVUT, Praha, 265 pp. (in Czech).

Polák, M. 2017. Experimental evaluation of hydraulic design modifications of radial centrifugal pumps. *Agronomy Research* **15**(S1), 1189–1197.

Polák, M. 2018. Determination of conversion relations for the use of small hydrodynamic pumps in reverse turbine operation. In: *Agronomy Research* **16** (S1), 1200–1208.

Pugliese, F., De Paola, F., Fontana, N., Giugni, M. & Marini, G. 2016. Experimental characterization of two pumps as turbines for hydropower generation. In: *Renewable energy*, **99**, 180–187.

Schmiedl, E. 1988. Series centrifugal pumps in turbine operation. Pump conference Karlsruhe, 357 p. (in German).

Sharma, K. 1985. Small hydroelectric project-use of centrifugal pumps as turbines. Technical report. Bangalore, India: Kirloskar Electric Co, pp. 14–26.

Singh, P. 2005. Optimization of the internal hydraulics and of system design for pumps as turbines with field implementation and evaluation. *Ph.D. thesis*. Germany: University of Karlsruhe.

Singh, P. & Nestmann, F. 2011. Internal hydraulic analysis of impeller rounding in centrifugal pumps as turbines. In: *Exp Therm Fluid Sci* **35**(No. 1), 121e34.

Stefanizzi, M., Torresi, M., Fortunato, B. & Camporeale, S.M. 2017. Experimental investigation and performance prediction modeling of a single stage centrifugal pump operating as turbine. In: *Energy Procedia*, Vol. **126**, pp 589–596.

Stepanoff, A.J. 1957. *Centrifugal and axial flow pumps, design and applications*, John Willy and Sons, Inc., New York, 462 pp.

Venturini, M., Alvisi, S., Simani, S. & Manservigi, L. 2017. Energy Production by Means of Pumps As Turbines in Water Distribution Networks. In: *Energies* **10**(10), 1666.

Williams, A.A. 1996. Pumps as turbines for low cost micro hydro power. In: *Renewable Energy* **9**(1–4), 1227–1234.

ČSN EN ISO 9906. 2013. Rotodynamic pumps - Hydraulic performance acceptance tests - Grades 1, 2 and 3, ČSNI (in Czech).